Cell Metabolism
Article

The Mitochondrial Chaperone TRAP1 Promotes Neoplastic Growth by Inhibiting Succinate Dehydrogenase

Marco Sciacovelli,[1,8] Giulia Guzzo,[1,8] Virginia Morello,[3] Christian Frezza,[4] Liang Zheng,[4,5] Nazarena Nannini,[2] Fiorella Calabrese,[2] Gabriella Laudiero,[6] Franca Esposito,[6] Matteo Landriscina,[7] Paola Defilippi,[3] Paolo Bernardi,[1,*] and Andrea Rasola[1,*]

[1]CNR Institute of Neuroscience, Department of Biomedical Sciences and Venetian Institute of Molecular Medicine
[2]Department of Cardiac, Thoracic and Vascular Sciences
University of Padova, 35121 Padova, Italy
[3]Molecular Biotechnology Centre, Department of Genetics, Biology and Biochemistry, University of Torino, 10125 Torino, Italy
[4]Cancer Research United Kingdom, The Beatson Institute for Cancer Research, Glasgow G61 1BD, UK
[5]Strathclyde Institute of Pharmacy and Biomedical Sciences, University of Strathclyde, Glasgow G61 1BD, UK
[6]Department of Molecular Medicine and Medical Biotechnologies, University of Napoli Federico II, 80131 Napoli, Italy
[7]Department of Medical and Surgical Sciences, University of Foggia, 71100 Foggia, Italy
[8]These authors contributed equally to this work
*Correspondence: bernardi@bio.unipd.it (P.B.), rasola@bio.unipd.it (A.R.)
http://dx.doi.org/10.1016/j.cmet.2013.04.019

SUMMARY

We report that the mitochondrial chaperone TRAP1, which is induced in most tumor types, is required for neoplastic growth and confers transforming potential to noncancerous cells. TRAP1 binds to and inhibits succinate dehydrogenase (SDH), the complex II of the respiratory chain. The respiratory downregulation elicited by TRAP1 interaction with SDH promotes tumorigenesis by priming the succinate-dependent stabilization of the proneoplastic transcription factor HIF1α independently of hypoxic conditions. These findings provide a mechanistic clue to explain the switch to aerobic glycolysis of tumors and identify TRAP1 as a promising antineoplastic target.

INTRODUCTION

Tumors undergo sustained growth in a dynamic environment where oxygen and nutrients are often scarce (Denko, 2008; Hanahan and Weinberg, 2011). To cope with the energetic requirements of rapid proliferation in these challenging conditions (Fritz and Fajas, 2010), tumor cells profoundly reorganize their core metabolism (Cairns et al., 2011; Levine and Puzio-Kuter, 2010). Glucose utilization, which provides ATP, essential anabolic intermediates, and antioxidative defenses (Hsu and Sabatini, 2008; Vander Heiden et al., 2009), is boosted and dissociated from oxygen availability (the Warburg effect; Warburg, 1956; Warburg et al., 1927). Key to the Warburg effect is the decrease of mitochondrial respiration (Frezza and Gottlieb, 2009), which allows cancer cells to grow in the hypoxic conditions found in the interior of the tumor mass (Hsu and Sabatini, 2008).

The molecular mechanisms that inhibit oxidative phosphorylation (OXPHOS) in tumors are understood only partially. The transcription factor HIF1 (hypoxia-inducible factor 1) decreases the flux of pyruvate into the Krebs cycle and, hence, the flow of reducing equivalents needed to power the electron transport chain (ETC) and stimulates glycolysis by inducing glucose transporters and glycolytic enzymes (Denko, 2008; Semenza, 2010b). HIF is activated by hypoxia as well as by the accumulation of the Krebs cycle metabolites succinate and fumarate that inhibit the prolyl hydroxylases (PHDs) responsible for proteasomal degradation of the HIF1α subunit (Selak et al., 2005). Succinate accumulation can originate from loss-of-function mutations in any of the genes encoding for succinate dehydrogenase (SDH) subunits (or their assembly factor SDHAF2), which cause hereditary paraganglioma-pheochromocytoma syndrome and are associated to a number of other neoplasms (Bardella et al., 2011).

Within this conceptual framework, we have analyzed the activity of TRAP1, an evolutionarily conserved chaperone of the Hsp90 family mainly located in the mitochondrial matrix and overexpressed in a variety of tumor cell types, where it exerts antiapoptotic functions through mechanisms that are only partially understood (Altieri et al., 2012; Kang et al., 2007). Our results indicate that TRAP1 supports tumor progression by downmodulating mitochondrial respiration through a decrease in the activity of SDH, which leads to HIF1α stabilization even in the absence of hypoxic conditions, by increasing succinate levels.

RESULTS

Mitochondrial TRAP1 Promotes Neoplastic Transformation

We found that TRAP1 is localized in mitochondria of cancer cell models (Figures S1A and S1B available online), as expected (Altieri et al., 2012), and that downregulation of TRAP1 expression by RNAi abrogated any transforming potential. In fact, knockdown of TRAP1 expression made SAOS-2 osteosarcoma cells, HCT116 colon carcinoma cells, and HeLa cervix carcinoma cells (dubbed shTRAP1 cells; Figures S1C–S1E) unable

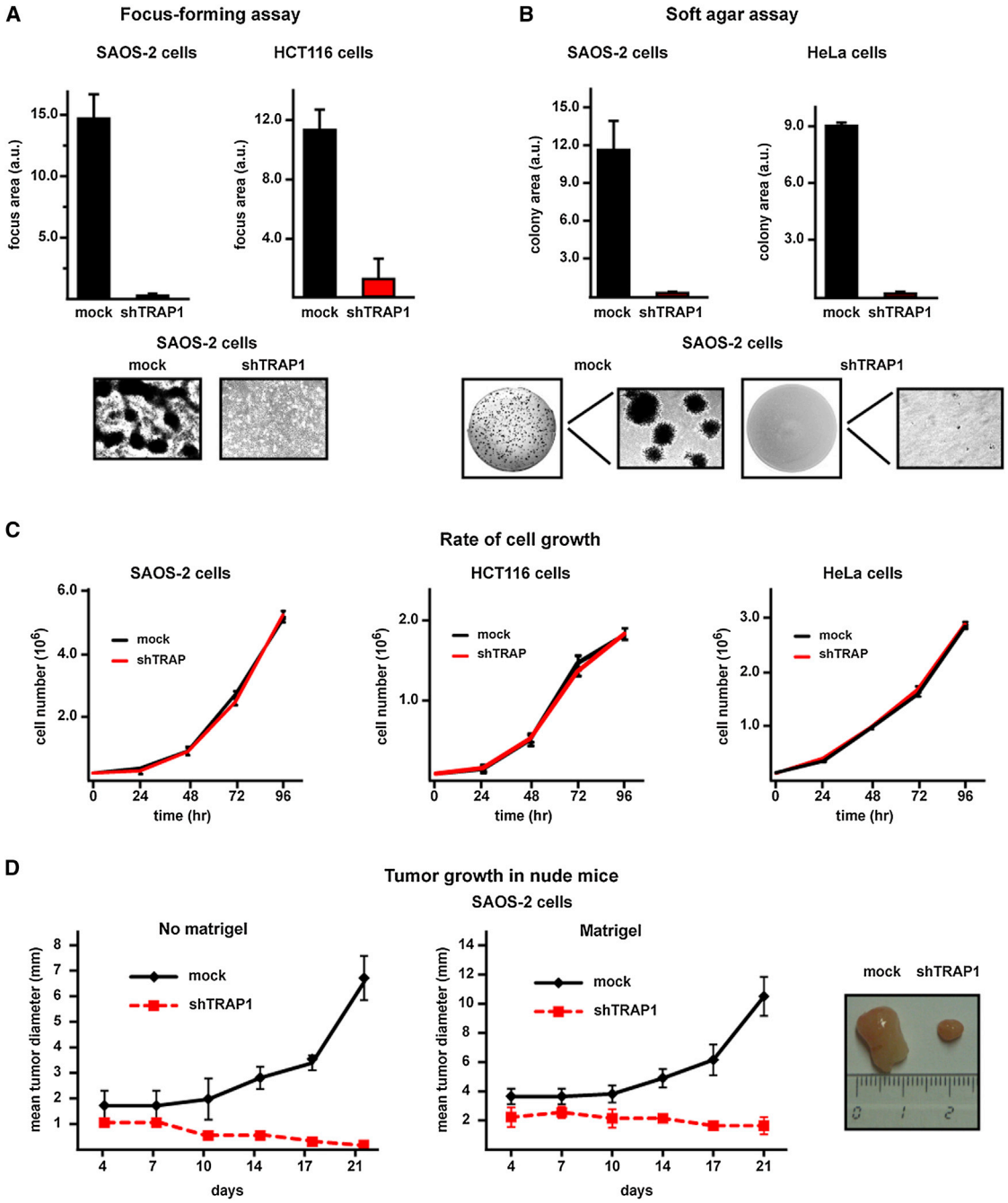

Figure 1. TRAP1 Knockdown Inhibits In Vitro and In Vivo Neoplastic Transformation

(A and B) Human osteosarcoma SAOS-2 cells, human colorectal carcinoma HCT116 cells, and human cervix carcinoma HeLa cells lose the capability to form foci (A) or colonies in soft agar (B) after knocking down TRAP1 expression. Cells stably transfected with a scrambled shRNA or with TRAP1 shRNAs are dubbed mock and shTRAP1, respectively. Data indicate the total focus or colony area at the 25th experimental day. Representative areas showing focus or colony growth are reported.

(C) Rate of growth of mock and shTRAP1 SAOS-2, HCT116, and HeLa cells.

(D) Kinetics of tumor growth in nude mice after injection of SAOS-2 cells without or with a Matrigel bolus (left and right, respectively); representative tumors grown with Matrigel are shown on the right. Data are reported as mean ± SD values ($n \geq 3$).

to both form foci (Figure 1A) and grow in soft agar (Figure 1B) without affecting the rate of cell growth (Figure 1C). Notably, shTRAP1 tumor cells lost the ability to develop tumor masses when injected into nude mice (Figure 1D).

Conversely, when the TRAP1 complementary DNA (cDNA) was expressed in either RWPE-1 prostate epithelial cells or fibroblasts, these nontransformed cells acquired the capacity to form colonies in soft agar (Figures 2A and 2D), and downregulation of

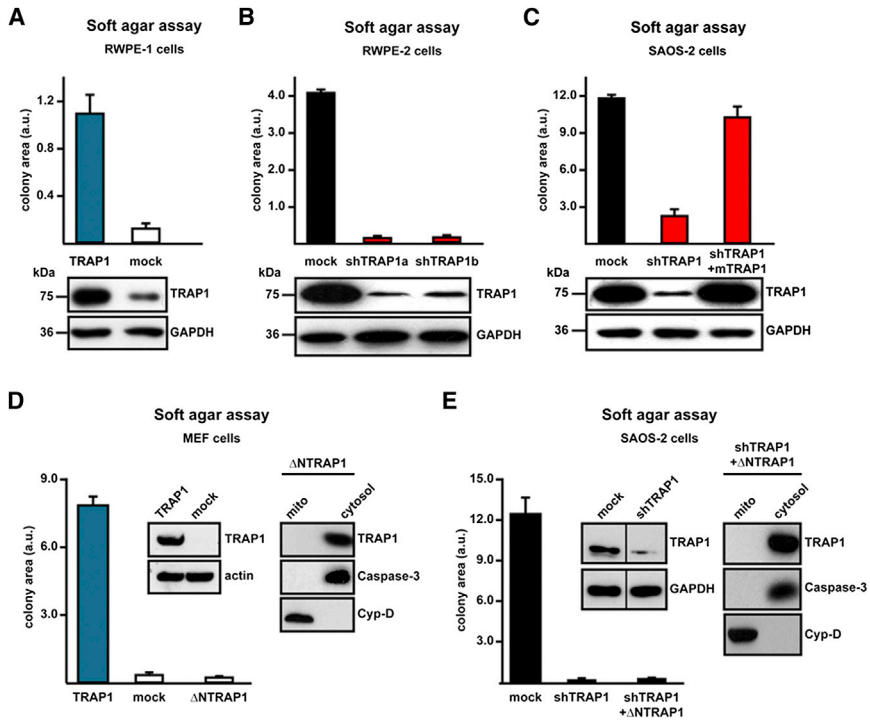

Figure 2. Mitochondrial TRAP1 Confers Transforming Potential to Cells

(A and B) Soft agar tumorigenesis assays were performed both in nontransformed cells (i.e., human epithelial prostate RWPE-1 cells) (A) and MEFs (D), stably transfected with either a TRAP1 cDNA or with a scrambled shRNA (mock); and in transformed cells, i.e., human epithelial prostate RWPE-2 cells obtained by *v*-Ki-Ras expression in RWPE-1 cells (B); cells dubbed shTRAP1a and shTRAP1b were transfected with different TRAP1 shRNAs.

(C) Expression of a mouse TRAP1 cDNA (mTRAP1) insensitive to human-directed shTRAP1 constructs reinstated the capability to form foci in human osteosarcoma SAOS-2 cells stably transfected with TRAP1 shRNAs (shTRAP1).

(D and E) Growth of colonies in soft agar was also assessed in MEF cells (D) or in SAOS-2 shTRAP1 cells (E) stably transfected with a TRAP1 construct lacking the mitochondrial import sequence (ΔNTRAP1). Western immunoblots show TRAP1 expression levels in the different cell types; GAPDH or actin are shown as loading controls. In (D) and (E), the cytosolic localization of ΔNTRAP1 was assessed by subcellular fractionation; caspase-3 and cyclophilin D (CyP-D) are used to verify purity of cytosolic and mitochondrial fractions, respectively. Data are reported as mean ± SD values ($n \geq 3$).

TRAP1 expression in RWPE-2 prostate cells, which are transformed by expression of v-Ki-Ras in RWPE-1 cells (Rasola et al., 2010a), abolished their tumorigenic features (Figure 2B). Moreover, stable transfection of a murine TRAP1 cDNA, which is insensitive to human-directed small hairpin RNA (shRNA) constructs, reinstalled the tumorigenic capability of shTRAP1 cells (Figure 2C). Mitochondrial localization of TRAP1 was essential for its proneoplastic activity, as expression of a TRAP1 cDNA devoid of its mitochondrial targeting sequence was not tumorigenic in either cancer or nontransformed cells (Figures 2D and 2E).

TRAP1 Binds SDH and Inhibits its Succinate:Coenzyme Q Reductase Enzymatic Activity

We then asked whether TRAP1 promotes transformation by acting on mitochondrial metabolism, thus contributing to the Warburg phenotype. This could occur through an inhibitory effect on respiration. We used a blue native (BN)-PAGE approach (Figure 3A), which allows the separation and characterization of protein complexes under nondenaturing conditions (Wittig and Schägger, 2008), to investigate a possible interaction between TRAP1 and ETC complexes. By cutting BN-PAGE bands and running them on an SDS-PAGE, we could observe the association between TRAP1 and both complex IV (cytochrome oxidase, COX) and complex II (succinate dehydrogenase, SDH) (Figure 3A). Moreover, by performing an immunoblot directly on the BN-PAGE, we found TRAP1 to be in correspondence with both complex IV and complex II bands; notably, these bands were diffused, and TRAP1 colocalized with their upper portion, suggesting that TRAP1 contributes to form a multimeric complex of higher molecular weight than the ETC complex per se (Figure 3B). We confirmed the interaction between TRAP1 and complex II/SDH through further approaches, including (1) immunoprecipitation, finding coimmunoprecipitation (coIP) of TRAP1 with SDH and vice versa (Figure 3C), and (2) mitochondrial protein crosslinking with dimethyl 3,3′-dithiobis-propionimidate (DTBP), a homobifunctional compound that reacts with the primary amines of two interacting proteins at an average distance of about 8 Å (Giorgio et al., 2009), followed by TRAP1 immunoprecipitation in order to determine whether TRAP1 and SDH are closely associated. We found that two TRAP1/SDH complexes are formed in mitochondria (Figure 3D).

We then measured whether TRAP1 affects complex II enzymatic activity. Complex II couples the Krebs cycle to OXPHOS by oxidizing succinate to fumarate and then transferring electrons to coenzyme Q; hence, the enzyme is called either SDH or succinate:coenzyme Q reductase (SQR; Cecchini, 2003; Lemarie and Grimm, 2011). SQR activity can be assessed spectrophotometrically in permeabilized mitochondria after inhibition of the other ETC complexes by recording the reduction of 2,6-dichlorophenolindophenol (DCPIP) in the presence of succinate as an electron donor and coenzyme Q1 as an intermediate electron acceptor. The slope of the absorbance decline of DCPIP is directly proportional to SQR activity (see Figure S2A). We found that SQR enzymatic activity was increased in mitochondria from shTRAP1 cells relative to those derived from control cells (Figures 4A, S2A, and S2B). TRAP1 did not affect either the cytochrome oxidase enzymatic activity of complex IV (Figure S2C) or complex II protein levels (Figure S2D) or mitochondrial mass (Figure S2E). Specificity of TRAP1 inhibition on SDH was assessed by (1) expression of the mouse TRAP1 (in shTRAP1 cells) that is insensitive to human-directed shTRAP1 constructs, which resulted in inhibition of SQR activity to values similar to those of mock cells (Figure 4A), and (2) using an inhibitor of

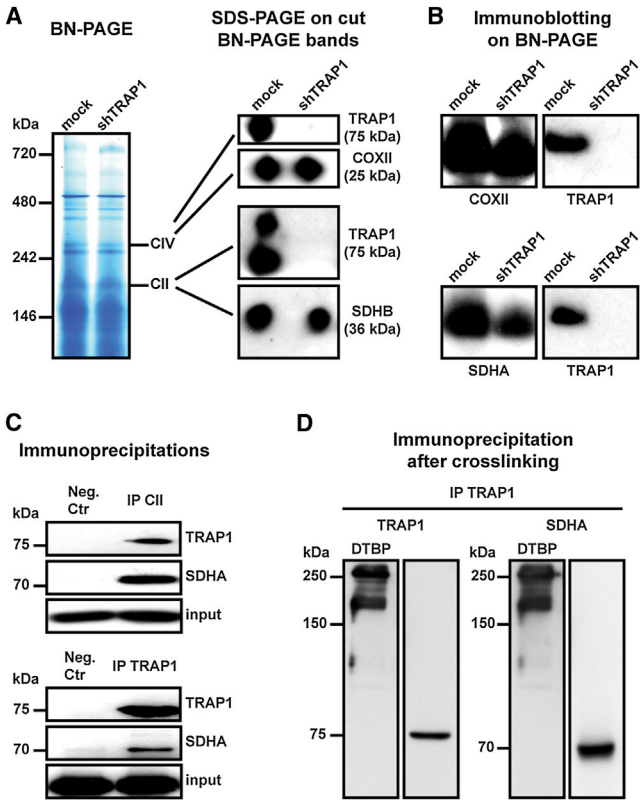

Figure 3. TRAP1 Binds to ETC Complexes IV and II

(A) Blue native gel electrophoresis. Bands corresponding to complex IV (cytochrome oxidase, COX) and complex II (succinate dehydrogenase, SDH) were cut, run on a SDS-PAGE, and probed with anti-TRAP1, anti-COX subunit II (COXII), and anti-SDH subunit B (SDHB) antibodies.

(B) Western immunoblotting was performed directly on a BN-PAGE. Probing was carried out with an anti-TRAP1 antibody and, in parallel lanes, with either an anti-COXII or an anti-SDH subunit A (SDHA) antibody. Note the smeared signal of both COXII and SDHA, suggesting that a population of complexes II and IV is present in the BN-PAGE; TRAP-1 is in the upper part of each complex band.

(C) Complex II and TRAP1 immunoprecipitations (IPs) on lysates of SAOS-2 mock cells. The interaction between TRAP1 and SDHA is shown by coIP. Immunoglobulin G (IgG) is used in negative isotype controls.

(D) Crosslinking experiments on mitochondria from mock SAOS-2 cells. TRAP1 was immunoprecipitated after mitochondrial treatment with the crosslinker DTBP, loaded in parallel on separate lanes of an SDS-PAGE, and probed with either an anti-TRAP1 or an anti-SDHA antibody.

TRAP1/Hsp90 ATPase activity (Felts et al., 2000), 17-allylamino-17-demethoxygeldanamycin (17-AAG), whose availability to mitochondria was recently shown in situ (Xie et al., 2011); 17-AAG specifically increased SQR activity in control mitochondria, whereas shTRAP1 mitochondria were insensitive to the drug (Figures 4A, 4B, and S2B). Notably, the effect of 17-AAG was unrelated to Hsp90, as Hsp90 protein levels were the same in mock and shTRAP1 cells (Figure S2F). The SQR activity of ETC complex II was further inhibited in mitochondria from control cells that progressed through the focus-forming assay compared to mitochondria from the same cells kept in standard culture conditions, whereas no change in SQR activity could be appreciated in mitochondria from shTRAP1 cells during the focus-forming experiments (Figure 4B). 17-AAG could still reactivate the SDH enzyme in mitochondria of TRAP1-expressing cells undergoing the focus-forming process (Figure 4B), indicating that even the enhanced inhibition of SQR activity occurring during the in vitro transformation progression is mediated by TRAP1 and remains reversible. In further accord with an inhibitory function of TRAP1 on ETC complex II, mitochondria from MEF cells stably expressing TRAP1 showed a diminished SQR activity compared to controls, and this inhibition was increased during the focus-forming assay; 17-AAG reactivated SDH selectively in mitochondria from TRAP1-expressing MEFs (Figure 4C).

TRAP1 Induction Inhibits Complex II Enzymatic Activity in Human Colorectal Cancers

TRAP1 expression was shown to be increased in a variety of tumor types (Kang et al., 2007 and http://www.proteinatlas.org/). We analyzed the SQR activity of ETC complex II in a set of human colorectal cancer samples and compared it with that measured in the surrounding nontransformed mucosa for each patient. In all colorectal cancer samples at stage IV, characterized by metastases to lymph nodes and to distant sites, and in the majority of samples of stage I–III, characterized by the absence of distant metastases, TRAP1 was upregulated relative to normal mucosa (Costantino et al., 2009). When we measured SQR activity in extracts from these samples, we found that TRAP1 upregulation was always paralleled by a decrease in SQR activity, and that this decrease could be partially rescued by adding 17-AAG before starting recordings (Figure 4D). In a small subset of stage I–III colorectal cancers, TRAP1 expression was not induced relative to surrounding nontumor tissues. In these samples, we could not detect any difference in SQR activity between samples from tumor and normal mucosa (Figure 4E), strengthening the link between TRAP1 and the regulation of complex II activity.

TRAP1 Inhibits Cell Oxygen Consumption Rate and ATP Production by OXPHOS

The SQR assays described so far measure the maximal enzymatic activity of complex II, as the complex is made accessible in permeabilized mitochondria and exposed to an excess of substrates. We next analyzed whether TRAP1 also affects the oxygen consumption rate (OCR) of living cells. Downregulation of TRAP1 markedly increased mitochondrial-dependent respiration in all cancer cell models we tested (Figures 5A, S3A, and S3B); in full accord with the effect of the drug on SQR activity (see Figure 4A), the TRAP1 inhibitor 17-AAG increased OCR only in TRAP1-expressing cells (Figure S4A). In shTRAP1 cells, the extra OCR was used to make ATP, as it was inhibited by the ATP synthase blocker oligomycin; moreover, addition of the uncoupler FCCP increased respiration well above the basal level, indicating an increased respiratory capacity that remained fully sensitive to ETC inhibition by rotenone (Figure 5A). The comparison with control cells is striking because, unlike shTRAP1 cells, they already utilize their maximal respiratory capacity under basal conditions, as shown by the lack of OCR increase with FCCP (Figure 5A), an arrangement implying that any additional ATP requirement must be provided by glycolysis. Consistently, we found that OXPHOS marginally contributes to ATP synthesis in mock cells, whereas a high proportion of the

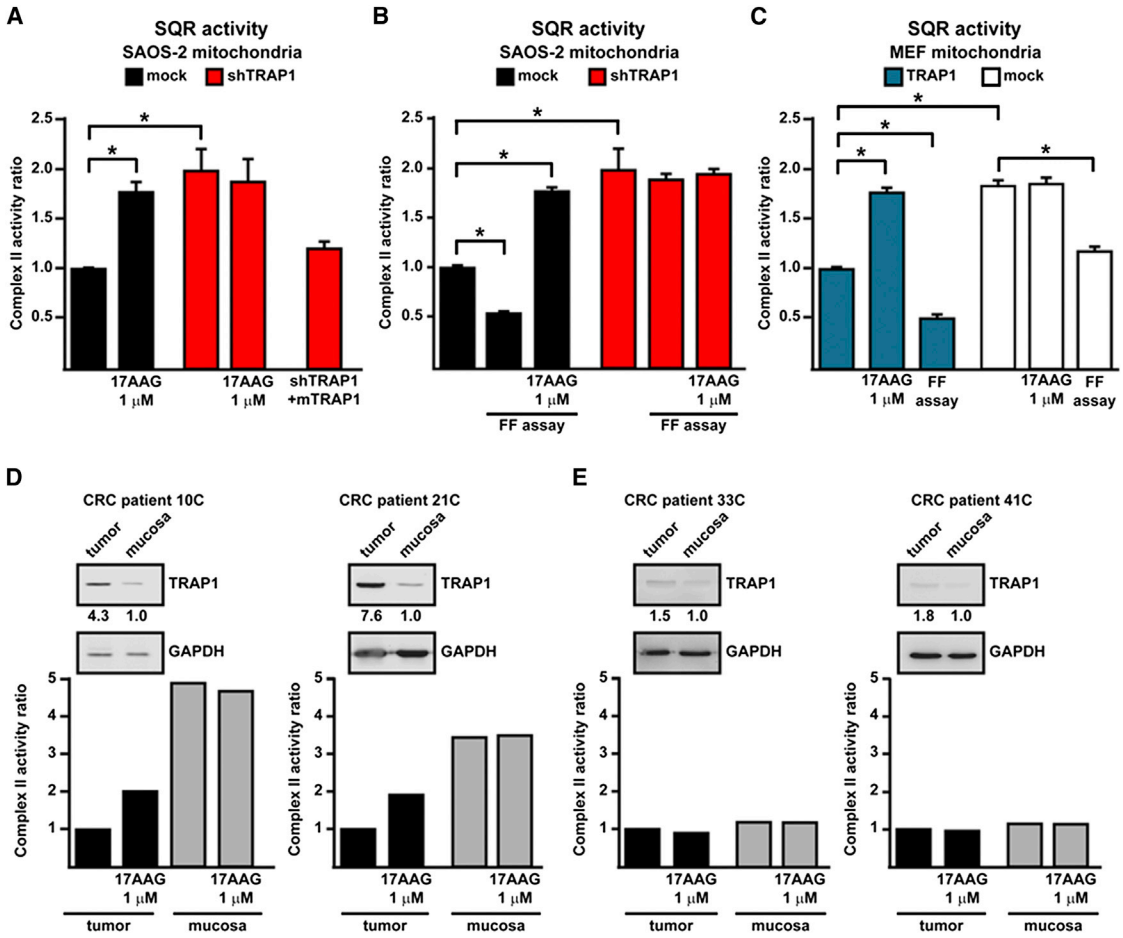

Figure 4. TRAP1 Downregulates the Enzymatic Activity of RC Complex II

(A and B) Analysis of the SQR enzymatic activity of complex II in mitochondria from SAOS-2 cells. In (A), analysis is performed on mitochondria from cultured cells; in (B), complex II activity values of mitochondria from cultured cells are compared with mitochondrial extracts from focus-forming assays obtained at the 15th experimental day (i.e., 1–2 days before cells that did not form foci massively underwent death). Mock indicates SAOS-2 cells stably transfected with a scrambled shRNA; shTRAP1 indicates SAOS-2 cells stably transfected with a TRAP1 shRNA; shTRAP1 + mTRAP1 indicates SAOS-2 shTRAP1 cells transfected with a mouse TRAP1 cDNA insensitive to human-directed shTRAP1 constructs (see Figure 2C). Enzyme activity values are compared to those of SAOS-2 mock cells in culture.

(C) SQR activity is measured on mitochondria from MEFs kept in culture or undergoing a focus-forming assay (15th day). TRAP1 indicates cells stably transfected with the TRAP1-containing vector; cells stably transfected with a control vector are dubbed mock. Enzyme activity values are compared to those of mitochondria from TRAP1-expressing MEFs in culture. TRAP1 inhibitor 17-AAG was added 5 min before starting recordings. Bar graphs report mean ± SD values ($n \geq 3$); *$p < 0.01$ with a Student's t test analysis.

(D and E) Representative analyses of SQR activity on human colorectal cancer (CRC) samples are compared to surrounding noncancerous mucosae of the same patient. As shown in the insets, TRAP1 expression was compared between each CRC and noncancerous mucosa by western immunoblot followed by densitometric analysis normalized to GAPDH, which was used as a loading control. TRAP1 was considered induced when the ratio of the protein level between tumor sample and surrounding noncancerous mucosa was ≥ 3. Samples reported in (D) were obtained from metastatic CRC tumors and display an increase of TRAP1 expression in tumors with respect to mucosae; samples reported in (E) were obtained from nonmetastatic CRC tumors and do not show any relevant increase of TRAP1 expression.

intracellular ATP content is provided by glycolysis, with a marked increase of glycolytic ATP during the in vitro tumorigenic process; instead, in shTRAP1 cells, most of the ATP comes from OXPHOS (Figure 5B). Moreover, expression of the TRAP1 cDNA in nontransformed fibroblasts markedly inhibited basal OCR and abolished any respiratory reserve (Figure 5C), mimicking the respiratory pattern of TRAP1-expressing tumor cells. Expression in shTRAP1 cells of the murine TRAP1 insensitive to human-directed shTRAP1 constructs determined an OCR pattern indistinguishable from that of mock cells (Figure 5D).

SDH Inhibitors Selectively Affect Respiration, Survival, and Soft Agar Growth in shTRAP1 Cells

A low concentration of the ETC complex II inhibitors 3-nitropropionic acid (3-NP), which inactivates SDH after covalent binding with an Arg residue in the catalytic core of SDHA (Huang et al., 2006), or thenoyltrifluoroacetone (TTFA), which blocks electron transfer from succinate to coenzyme Q at the quinone-binding site in subunits B and D (Huang et al., 2006), inhibited OCR in shTRAP1 cells but were inactive in the presence of TRAP1 (Figures S4B and S4C), paralleling the downmodulation of the SQR

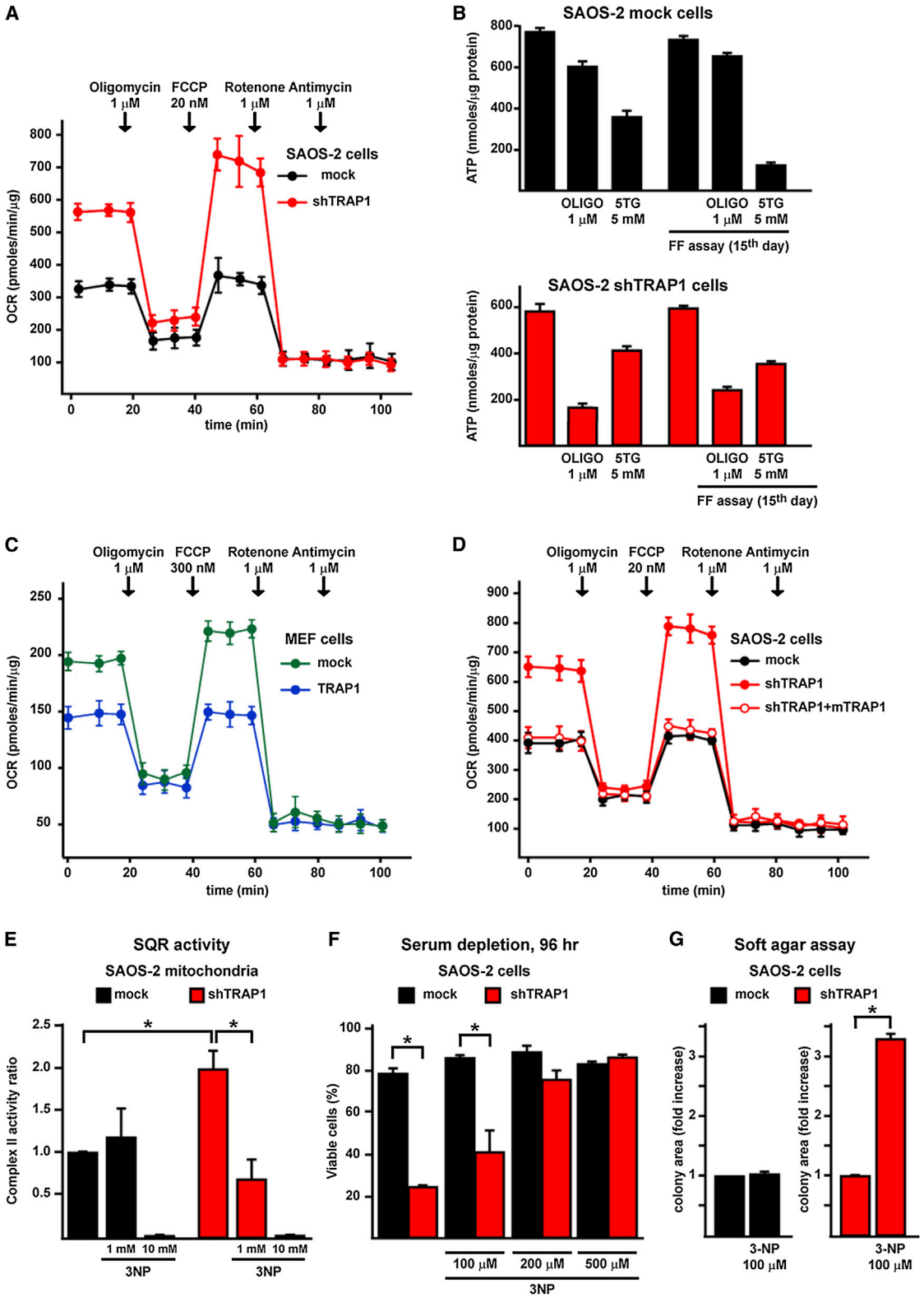

Figure 5. TRAP1-Induced Downmodulation of SDH Activity Decreases Cell Oxygen Consumption Rate and OXPHOS-Dependent Synthesis of ATP and Prompts Resistance to Stress Stimuli

(A) Representative traces of OCR experiments performed on monolayers of living SAOS-2 cells. Subsequent additions of the ATP synthase inhibitor oligomycin, the uncoupler FCCP, the ETC complex I inhibitor rotenone, and the ETC complex III inhibitor antimycin A were carried out.

(legend continued on next page)

activity induced by 3-NP only in TRAP1-expressing mitochondria (Figure 5E). These data indicate that TRAP1 limits maximal respiration by acting at ETC complex II. We also found that 3-NP inhibits death in a dose-dependent fashion in shTRAP1, but not in mock SAOS-2 cells placed in conditions of long-term starvation that mimic the paucity of nutrients found in the inner tumor mass during the phases of its rapid accrual (Figure 5F). Moreover, treatment with 3-NP partially restored the ability of shTRAP1 cells to form colonies in soft agar, whereas it was ineffective on the colonies formed by control cells (Figure 5G).

TRAP1 Induces Succinate Accumulation and HIF1α Stabilization, which Is Required for Tumor Cell Growth

It was shown that succinate induces HIF1 by inhibiting PHDs, the enzymes that hydroxylate HIF1α, allowing its subsequent ubiquitin-dependent degradation (Selak et al., 2005). We observed that during the focus-forming assay, the intracellular level of succinate increased only in TRAP1-expressing cells (Figure 6A), matching the downmodulation of their SDH enzymatic activity (Figure 4B). In keeping with these results, HIF1α was detectable exclusively in TRAP1-expressing cells during the focus-forming process (Figure 6B), whereas it was hydroxylated on Pro residues (i.e., primed for proteasomal degradation) both in culture conditions, independently of the presence of TRAP1, and in shTRAP1 cells exposed to focus-forming conditions (Figure 6C). HIF2α, which shares some redundant functions with HIF1α and whose expression is increased in a broad spectrum of cancer cell types (Keith et al., 2012), was not stabilized in our experimental conditions (Figure 6D). We then used pimonidazole, a compound that is reductively activated under hypoxic conditions and forms protein adducts by reacting with Cys residues (Arteel et al., 1998), to understand whether HIF1α stabilization could at least partially depend on hypoxic conditions occurring during the formation of foci. Remarkably, we could not detect any induction of pimonidazole-protein adducts in TRAP1-expressing cells during the process of in vitro tumorigenesis, even when HIF1α had already been stabilized (Figure 6E), which demonstrates that pseudohypoxic conditions elicited by the presence of TRAP1 are sufficient to promote HIF1α stabilization. Tumor samples obtained from nude mice xenografted with TRAP1-expressing SAOS-2 cells (see Figure 1D) were characterized by densely packed cells, amidst which fibrotic and necrotic areas could be observed (Figure 6F, marked as F and N, respectively); HIF1α was clearly detected in the majority of cells, the signal being particularly strong in the nuclei of cells where proliferation markers were also evident (compare the MIB/Ki67 and the HIF1α staining in Figure 6F). In these samples, cells displayed a punctate TRAP1 signal that fits well with its mitochondrial localization (see the high-magnification TRAP1 staining in Figure 6F). The addition of dimethyl succinate, a membrane-permeable succinate analog, to the focus-forming culture medium both stabilized HIF1α (Figure 7A) and rescued the capability to form colonies (Figure 7B) in shTRAP1 cells, while it did not further increase the tumorigenicity of TRAP1-expressing cells (Figure 7B). Moreover, HIF1α inhibition either with a cell-permeable esterified form of α-ketoglutarate (1-trifluoromethylbenzyl-α-ketoglutarate, TaKG), which reverses HIF1α stabilization by restoring PHD enzymatic activity (MacKenzie et al., 2007; Tennant et al., 2009), or with RNAi on HIF1α or HIF1β, the latter being the stable subunit of the heterodimeric HIF transcription factors (Keith et al., 2012), fully abolished formation of foci in TRAP1-expressing tumor cells and in MEFs transfected with a TRAP1 cDNA (Figures 7C–7F). Taken together, these data indicate that TRAP1 prompts neoplastic growth by inducing a succinate-dependent stabilization of HIF1α.

DISCUSSION

Tumor cells tend to increase their glycolytic activity without a matching increase of oxidative phosphorylation (Warburg, 1956; Warburg et al., 1927). Inhibition of the tumor suppressor p53 or activation of the transcription factor HIF1 curtails OXPHOS by inducing the autophagic degradation of respiratory complexes and by abrogating the synthesis of some of their subunits (such as SDHB) or assembly factors (Denko, 2008; Semenza, 2010a; Vousden and Ryan, 2009). Conversely, OXPHOS inhibition can play a causal role in tumorigenesis. Inactivating mutations in mitochondrial DNA (mtDNA) genes encoding for subunits of ETC complexes I and III were found associated with renal oncocytomas (Gasparre et al., 2008) as well as thyroid and prostate cancers (Abu-Amero et al., 2005; Petros et al., 2005). However, these mutations are confined to a small set of neoplasms, and the lack of clear-cut molecular mechanisms hampers the definition of whether OXPHOS inhibition as such can play a general tumorigenic role. Key findings of the present work demonstrate that the mitochondrial chaperone TRAP1, which is widely expressed in most tumors, but

(B) ATP levels were measured in mock or shTRAP1 SAOS-2 cells kept in standard culture conditions (bars on the left) or in a focus-forming assay for 15 days (i.e., 1–2 days before cells that did not form foci massively underwent death (bars on the right). Where indicated, cells were treated for 2 hr with the ATP synthase inhibitor oligomycin or the hexokinase inhibitor 5-thioglucose (5TG) in a no-glucose medium to discriminate between ATP produced by OXPHOS and by glycolysis.
(C and D) Representative traces of OCR experiments performed on monolayers of living MEF cells (C) or SAOS-2 cells (D). Experiments were carried out as in (A).
(E) Analysis of the effect of the SDH inhibitor 3-NP on the SQR enzymatic activity of complex II in mitochondria from SAOS-2 cells. 3-NP was added 5 min before starting recordings; 10 mM 3-NP was used to fully inhibit the SDH enzyme.
(F) Cytofluorimetric cell death analysis of SAOS-2 cells starved in a medium without serum for 96 hr with or without the reported concentrations of 3-NP. Viable cells are identified as double negative for propidium iodide and Annexin V-FITC.
(G) Soft agar assay on SAOS-2 cells. Data are reported as fold increase of colony area of mock cells grown with 3-NP compared with mock cells kept without the drug (left) and, separately, as fold increase of colony area of shTRAP1 cells grown with 3-NP compared with shTRAP1 cells kept without the drug (right). In SAOS-2 experiments, mock indicates cells stably transfected with a scrambled shRNA; shTRAP1 indicates cells stably transfected with a TRAP1 shRNA; shTRAP1 + mTRAP1 indicates cells stably transfected with a TRAP1 shRNA and expressing a mouse TRAP1 cDNA. In the experiment with MEFs, cells were stably transfected with either a TRAP1 cDNA or a scrambled shRNA (mock). All bar graphs report mean ± SD values ($n \geq 3$); $^*p < 0.01$ with a Student's t test analysis.

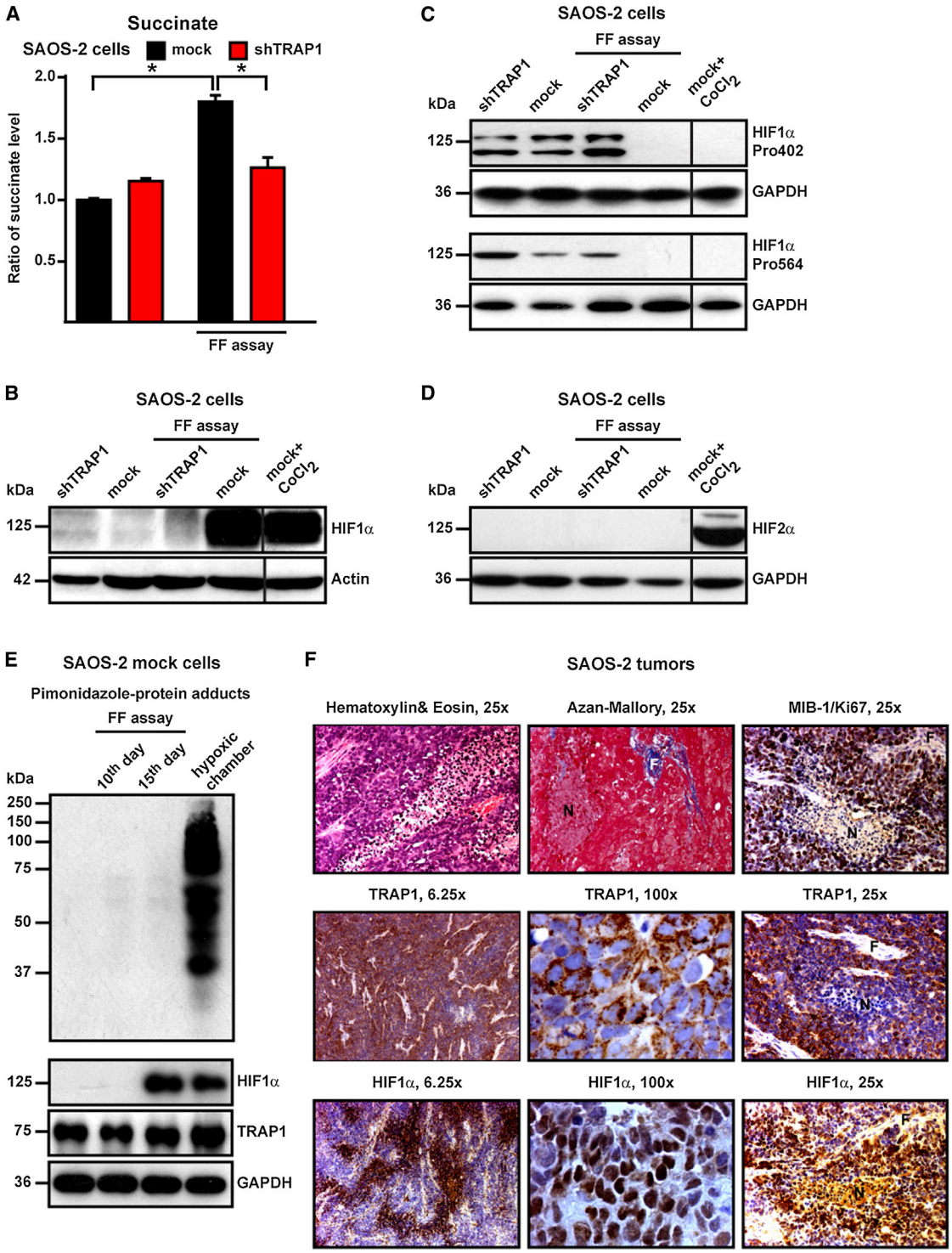

Figure 6. TRAP1 Increases Intracellular Succinate Concentration and Stabilizes HIF1α in a Hypoxia-Independent Way

(A) Bar graphs showing liquid chromatography-mass spectrometry (LC-MS) measurements of intracellular succinate level. Values are compared with cultured mock SAOS-2 cells.

(B–D) Western immunoblots showing HIF1α expression (B), HIF1α hydroxylation of the Pro402 and Pro564 residues (C), and HIF2α expression in cultured cells and on extracts from focus-forming assays obtained at the 15th experimental day (i.e., 1–2 days before cells that did not form foci massively underwent death). $CoCl_2$ is used as a positive control for HIF1α and HIF2α stabilization. Blots were probed with an anti-actin (B) or an anti-GAPDH (C and D) antibody to check for protein load.

(E) Detection of pimonidazole-protein adducts in SAOS-2 mock cells kept in either normal culture or focus-forming conditions for 10 or 15 days. Pimonidazole (200 μM) was added on the focus-forming plate 2 hr before lysis. As a positive control, cells were kept for 24 hr in a hypoxic chamber (0.5% O_2). On

(legend continued on next page)

not in highly proliferating, nontransformed cells (http://www.proteinatlas.org/), is a component of the molecular machinery that decreases mitochondrial respiration and that this event is crucial for neoplastic progression. Indeed, we find that TRAP1 behaves as an oncogene since (i) without TRAP1, tumorigenesis is blunted both in vitro and in vivo, and (ii) TRAP1 expression confers tumorigenic potential to nontransformed cells. We observe that TRAP1-mediated inhibition of SDH limits the maximal rate of respiration and leads to succinate accumulation followed by HIF1α, but not HIF2α, stabilization. Remarkably, the membrane-permeable succinate analog dimethyl succinate could both elicit HIF1α stabilization and rescue the tumorigenic phenotype of shTRAP1 cells, highlighting the mechanistic connection between TRAP1-dependent succinate accumulation and HIF1α-dependent tumor formation.

The role played by the transcription factor HIF1 in tumorigenesis is complex. Once activated by inhibition of the proteasomal degradation of its α subunit (either HIF1α or HIF2α), and by the ensuing association with the stable β subunit (HIF1β), HIF1 can boost evolution of neoplasms by promoting angiogenesis, epithelial-mesenchymal transition, and the glycolytic switch (Brahimi-Horn et al., 2011; Semenza, 2010a). In multiple tumor models, both HIF1α and HIF2α promote neoplastic progression by regulating sets of genes that are only partially shared, and independent roles for HIF1α and HIF2α can depend on the cancer type or on its growth and progression stages (Keith et al., 2012). However, both α subunits can play a tumor suppressor function in specific tumor types, such as renal cell carcinoma (HIF1α) or lung adenocarcinoma (HIF2α), through poorly defined mechanisms. In our model, HIF1α stabilization, and the ensuing HIF activation, have a crucial proneoplastic role, as promoting HIF1α degradation or knocking down either HIF1α or HIF1β abolishes the neoplastic potential of TRAP1-expressing cells. Instead, we could not observe any HIF2α stabilization, ruling out its role in the TRAP1-dependent tumorigenic process. It is interesting that HIF2α accumulates at higher O_2 concentrations than HIF1α (Keith et al., 2012), and the possibility exists that, at variance with what we observe for HIF1α, pseudohypoxic conditions are insufficient or unable to stabilize HIF2α.

HIF1α stabilization emerges after several days of in vitro transformation. This is not at all surprising because excess succinate can be utilized in multiple pathways, including increased heme synthesis (Frezza et al., 2011), and because SDH becomes more strongly inhibited by TRAP1 during the focus-forming assay. The latter observation also suggests that a threshold SDH inhibition must be reached to allow for succinate accumulation. Despite a partial respiratory inhibition, TRAP1-expressing cells fully utilize their residual respiratory capacity to produce ATP, as shown by OCR experiments, but reorient their metabolism toward glycolysis to meet any energy demand that exceeds respiratory capacity, in complete accord with Warburg's observations.

TRAP1 is likely to begin a feedforward loop, as it inhibits SDH and respiration (hence OXPHOS) and induces HIF1, which in turn further inhibits OXPHOS (Denko, 2008; Semenza, 2010b) and directly downregulates SDH by induction of miR-210 (Puissségur et al., 2011). Notably, we have determined that TRAP1-dependent stabilization of HIF1α occurs in a pseudohypoxic way (i.e., in the absence of any hypoxic stress). This observation has potential implications for the kinetics of tumor development, as TRAP1 could induce HIF1 transcriptional activity even before the dysregulated accrual of the tumor mass creates hypoxic areas in its inner core.

At variance with the complete block of the SDH enzyme, which is an extreme case caused by loss-of-function mutations only seen in specific subsets of tumors (Bardella et al., 2011), the partial and reversible SDH inhibition caused by TRAP1 and its increased expression levels would mediate a more general proneoplastic function, which fits with TRAP1 identification as a bona fide inducible target of the proto-oncogene c-Myc (Coller et al., 2000).

Tumor cells could be endowed with a multichaperone mitochondrial complex, as TRAP1 interacts with cyclophilin D, Hsp90, and Hsp60 (Ghosh et al., 2010; Kang and Altieri, 2009). Given the multiplicity of chaperone client proteins, we cannot exclude further interactions of TRAP1 with other mitochondrial components. For instance, TRAP1 is involved in the inhibition of the mitochondrial permeability transition pore (Kang et al., 2007), whose opening irreversibly commits cells to death (Rasola and Bernardi, 2007; Rasola et al., 2010b), and we have observed that keeping the pore locked can be used by tumor cells to evade apoptosis (Rasola et al., 2010a). Thus, TRAP1 could take part in several mitochondrial changes that crucially contribute to the neoplastic phenotype. Targeting its chaperone activity and molecular interactors could dismantle the metabolic and survival adaptations of neoplastic cells, paving the way to the development of highly selective, mitochondriotropic antineoplastic drugs.

EXPERIMENTAL PROCEDURES

Detailed methods can be found in the Supplemental Experimental Procedures.

Cell Cultures and Tissue Samples

Experiments were performed on different cell models: human SAOS-2 osteosarcoma cells, human HCT116 colorectal carcinoma cells, RWPE1/RWPE2 prostate epithelial cells, HeLa cervix carcinoma cells, and MEFs. TRAP1, HIF1α, and HIF1β expression was knocked down by stable transfections with shRNAs. Cells transfected with scrambled shRNA were always used as controls. TRAP1 re-expression in interfered human cells was obtained by using a mouse cDNA. Stable transfection of a TRAP1 cDNA was performed in MEF cells that show negligible levels of the endogenous protein. Tissue

the same samples, both HIF1α stabilization and the expression level of TRAP1 were evaluated; blots were probed with an anti-GAPDH to check for protein load.

(F) Immunohistochemical inspections of tumors formed by SAOS-2 control cells after injection in nude mice (see Figure 1F). Hematoxylin and eosin (H&E) and Azan-Mallory staining reveal tumors rich in densely packed cells, with few fibrotic areas (F) and a large number of necrotic regions (N). TRAP1 is visible in most cells (see the 6.25× magnification) as a punctate signal (100× magnification), which is compatible with its mitochondrial localization. HIF1α expression is evident all along the samples (see the 6.25× magnification), mainly in the nuclear compartment of cells (100× magnification), and the signal is particularly strong in the perinecrotic areas, where the proliferation marker MIB-1/Ki67 is also found (25× magnification).

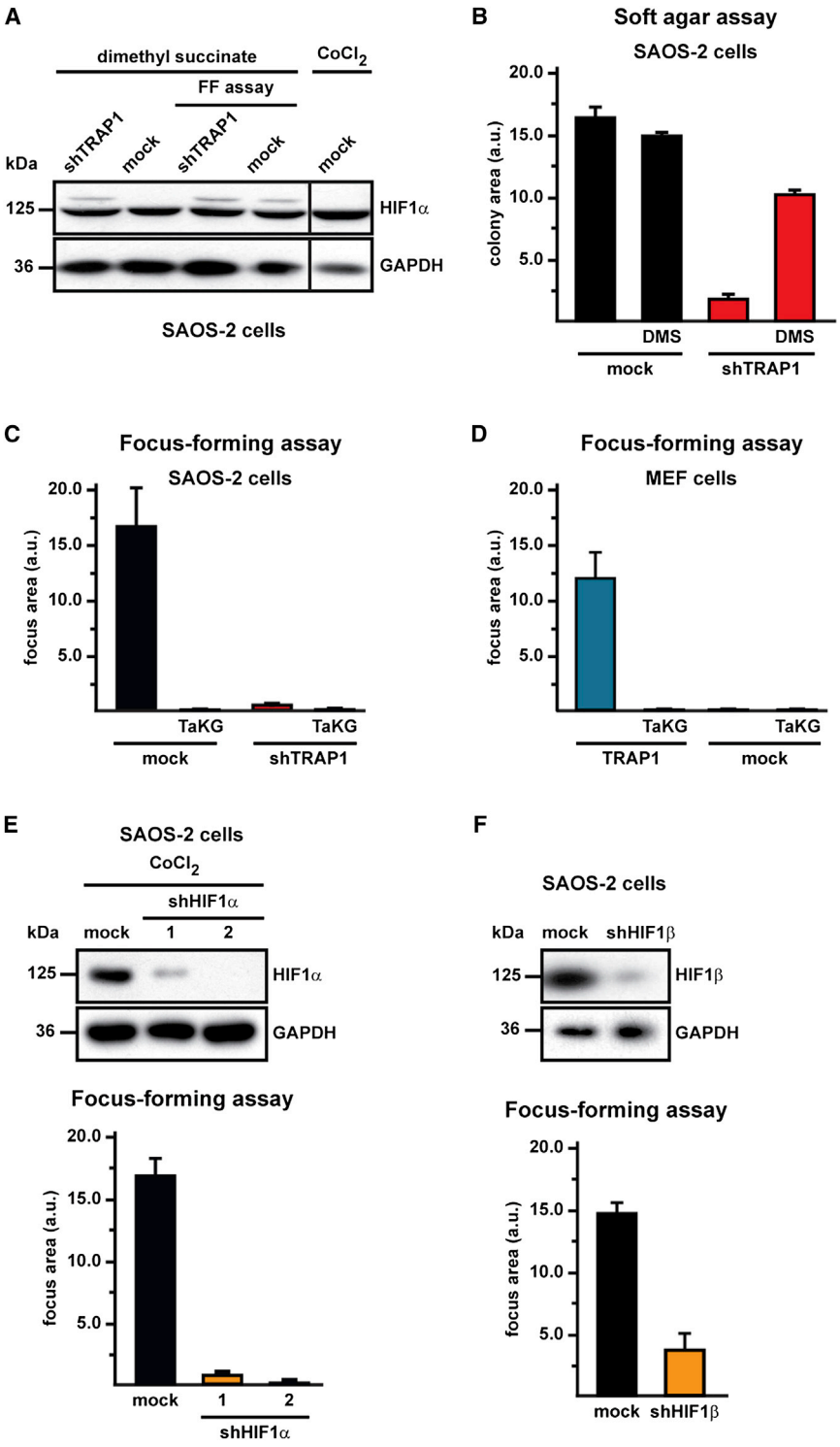

Figure 7. TRAP1 Favors Tumor Growth through Succinate-Dependent Stabilization of HIF1α

(A) Western immunoblot showing HIF1a stabilization in SAOS-2 cells kept either in culture or in focus-forming conditions in the presence of the cell-permeable succinate analog dimethyl succinate (20 mM, 48 hr). Extracts from focus-forming assays were obtained at the 15th experimental day (i.e., 1–2 days before cells that did not form foci massively underwent death). Blots were probed with an anti-GAPDH to check for protein load. Cells are dubbed as in previous figures with respect to TRAP1 expression.

(B) Soft agar experiments performed on SAOS-2 cells treated with dimethyl succinate (5 mM). Data indicate the total colony area at the 25th experimental day.

(C–F) Focus-forming assays on SAOS-2 cells (C) or MEFs (D) grown with or without TaKG and on SAOS-2 cells in which HIF1α (E) or HIF1β (F) expression had been knocked down by RNAi. Data are reported as in Figure 1A. In (E), $CoCl_2$ treatment is used to maximize HIF1α expression. In (F), knocking down of HIF1β is obtained with a mixture of three different shRNAs. Bar graphs report mean ± SD values ($n \geq 3$); *$p < 0.01$ with a Student's t test analysis. Cells are dubbed as in previous figures.

samples from both tumor and normal, noninfiltrated peritumoral mucosa were obtained from patients with colorectal carcinoma during surgical cancer removal after express written informed consent was obtained from all patients.

Tumorigenesis Assays

Three different tumorigenesis assays were performed: (1) focus-forming assays, in which cells were grown to confluence and kept in culture for the subsequent 25 days; tumor cells lose contact inhibition and overgrow to form foci; (2) soft agar assays, in which cells are embedded in an agar matrix; only transformed cells, which escape anoikis death signals, can grow to form colonies; (3) cell injection in nude mice, in order to follow the growth of primary tumors. Samples obtained from these assays were also exploited for investigating changes in complex II enzymatic activity in succinate levels and in HIF1α stabilization and distribution.

Cytofluorimetric Analyses

Cytofluorimetric analyses were utilized to analyze cell death induction with the use of Annexin V-FITC and propidium iodide probes as well as mitochondrial mass with the use of N-acridine orange.

Mitochondria Purification

Mitochondria were isolated through sequential centrifugations after mechanical cell disruption. In order to establish submitochondrial protein localization, isolated mitochondria were partially digested with different concentrations of trypsin.

Western Immunoblots and Immunoprecipitations, BN-PAGE, and Crosslinkings

Western immunoblot and immunoprecipitation experiments were performed following standard techniques. BN-PAGE experiments were carried out on isolated mitochondria in order to identify ETC complexes. After a first electrophoresis in nondenaturing conditions, bands were visualized with Coomassie blue staining, cut, and run on SDS-PAGE for the identification of protein components by western immunoblot. Crosslinking assays were performed on isolated mitochondria incubated with the membrane-permeable, homobifunctional reagent DTBP prior to TRAP1 immunoprecipitation.

ETC Complex II Activity Assays and Oxygen Consumption Rate Experiments

Complex II enzymatic activity was investigated, measuring the SQR activity with classical spectrophotometric approaches on cell or tumor lysates. Complex IV enzymatic activity was investigated, measuring the oxidation of reduced cytochrome *c*. Each measurement of the respiratory chain (RC) complex activity was normalized for protein amount and for citrate synthase activity. In vivo respiration was followed in a kinetic mode by measuring the oxygen consumption rate (OCR) of cell monolayers with an extracellular flux analyzer.

Immunohistochemical and Immunoelectron Microscopy Analyses

Immunohistochemical inspections were performed on serial sections of paraffin-embedded tumor samples obtained from xenografted nude mice following standard procedures. Immunoelectron microscopy (immuno-EM) inspections were performed on antibody-labeled fixed cells using the gold-enhanced protocol.

Determination of Intracellular Succinate Level

Intracellular succinate level was analyzed on lysates obtained by scraping cells placed in a cold methanol/acetonitrile solution. After spinning down the insoluble material, the supernatant was collected, and metabolites were separated using a liquid chromatography system coupled online to an LTQ Orbitrap mass spectrometer equipped with an electrospray ionization source.

Intracellular ATP Determination

Intracellular ATP was quantified by the luciferin/luciferase method. Cells were kept for 2 hr in the different experimental conditions.

Statistical Analysis

Student's t test was used to compare pairs of data groups. In all figures, bar graphs report mean ± SD values ($n \geq 3$); $^{*}p < 0.05$.

SUPPLEMENTAL INFORMATION

Supplemental Information includes Supplemental Experimental Procedures and four figures and can be found with this article online at http://dx.doi.org/10.1016/j.cmet.2013.04.019.

ACKNOWLEDGMENTS

We thank Eyal Gottlieb, Stefano Indraccolo, and Valentina Giorgio for insightful discussions; Matteo Curtarello and Luca Persano for help with hypoxic chamber experiments; Roman S. Polishchuk for electron microscopy analyses; Elena Trevisan for technical assistance; and our system operators Otello Piovan and Marco Ardina for inexhaustible help. This work was supported by grants from Progetto Strategico di Ateneo dell'Università di Padova ("Models of Mitochondrial Diseases"), Associazione Italiana Ricerca sul Cancro (grant number 8722), Ministero Istruzione Università Ricerca (Fondo per gli Investimenti della Ricerca di Base (grant number RBAP11S8C3), and Telethon (grant numbers GGP 11082 and GPP100005A). The work performed by C.F. and L.Z. was supported by Cancer Research UK.

Received: September 24, 2012
Revised: February 14, 2013
Accepted: April 5, 2013
Published: June 4, 2013

REFERENCES

Abu-Amero, K.K., Alzahrani, A.S., Zou, M., and Shi, Y. (2005). High frequency of somatic mitochondrial DNA mutations in human thyroid carcinomas and complex I respiratory defect in thyroid cancer cell lines. Oncogene *24*, 1455–1460.

Altieri, D.C., Stein, G.S., Lian, J.B., and Languino, L.R. (2012). TRAP-1, the mitochondrial Hsp90. Biochim. Biophys. Acta *1823*, 767–773.

Arteel, G.E., Thurman, R.G., and Raleigh, J.A. (1998). Reductive metabolism of the hypoxia marker pimonidazole is regulated by oxygen tension independent of the pyridine nucleotide redox state. Eur. J. Biochem. *253*, 743–750.

Bardella, C., Pollard, P.J., and Tomlinson, I. (2011). SDH mutations in cancer. Biochim. Biophys. Acta *1807*, 1432–1443.

Brahimi-Horn, M.C., Bellot, G., and Pouysségur, J. (2011). Hypoxia and energetic tumour metabolism. Curr. Opin. Genet. Dev. *21*, 67–72.

Cairns, R.A., Harris, I.S., and Mak, T.W. (2011). Regulation of cancer cell metabolism. Nat. Rev. Cancer *11*, 85–95.

Cecchini, G. (2003). Function and structure of complex II of the respiratory chain. Annu. Rev. Biochem. *72*, 77–109.

Coller, H.A., Grandori, C., Tamayo, P., Colbert, T., Lander, E.S., Eisenman, R.N., and Golub, T.R. (2000). Expression analysis with oligonucleotide microarrays reveals that MYC regulates genes involved in growth, cell cycle, signaling, and adhesion. Proc. Natl. Acad. Sci. USA *97*, 3260–3265.

Costantino, E., Maddalena, F., Calise, S., Piscazzi, A., Tirino, V., Fersini, A., Ambrosi, A., Neri, V., Esposito, F., and Landriscina, M. (2009). TRAP1, a novel mitochondrial chaperone responsible for multi-drug resistance and protection from apoptotis in human colorectal carcinoma cells. Cancer Lett. *279*, 39–46.

Denko, N.C. (2008). Hypoxia, HIF1 and glucose metabolism in the solid tumour. Nat. Rev. Cancer *8*, 705–713.

Felts, S.J., Owen, B.A., Nguyen, P., Trepel, J., Donner, D.B., and Toft, D.O. (2000). The hsp90-related protein TRAP1 is a mitochondrial protein with distinct functional properties. J. Biol. Chem. *275*, 3305–3312.

Frezza, C., and Gottlieb, E. (2009). Mitochondria in cancer: not just innocent bystanders. Semin. Cancer Biol. *19*, 4–11.

Frezza, C., Zheng, L., Folger, O., Rajagopalan, K.N., MacKenzie, E.D., Jerby, L., Micaroni, M., Chaneton, B., Adam, J., Hedley, A., et al. (2011). Haem oxygenase is synthetically lethal with the tumour suppressor fumarate hydratase. Nature *477*, 225–228.

Fritz, V., and Fajas, L. (2010). Metabolism and proliferation share common regulatory pathways in cancer cells. Oncogene *29*, 4369–4377.

Gasparre, G., Hervouet, E., de Laplanche, E., Demont, J., Pennisi, L.F., Colombel, M., Mège-Lechevallier, F., Scoazec, J.Y., Bonora, E., Smeets, R., et al. (2008). Clonal expansion of mutated mitochondrial DNA is associated with tumor formation and complex I deficiency in the benign renal oncocytoma. Hum. Mol. Genet. *17*, 986–995.

Ghosh, J.C., Siegelin, M.D., Dohi, T., and Altieri, D.C. (2010). Heat shock protein 60 regulation of the mitochondrial permeability transition pore in tumor cells. Cancer Res. *70*, 8988–8993.

Giorgio, V., Bisetto, E., Soriano, M.E., Dabbeni-Sala, F., Basso, E., Petronilli, V., Forte, M.A., Bernardi, P., and Lippe, G. (2009). Cyclophilin D modulates mitochondrial F0F1-ATP synthase by interacting with the lateral stalk of the complex. J. Biol. Chem. *284*, 33982–33988.

Hanahan, D., and Weinberg, R.A. (2011). Hallmarks of cancer: the next generation. Cell *144*, 646–674.

Hsu, P.P., and Sabatini, D.M. (2008). Cancer cell metabolism: Warburg and beyond. Cell *134*, 703–707.

Huang, L.S., Sun, G., Cobessi, D., Wang, A.C., Shen, J.T., Tung, E.Y., Anderson, V.E., and Berry, E.A. (2006). 3-nitropropionic acid is a suicide inhibitor of mitochondrial respiration that, upon oxidation by complex II, forms a covalent adduct with a catalytic base arginine in the active site of the enzyme. J. Biol. Chem. *281*, 5965–5972.

Kang, B.H., and Altieri, D.C. (2009). Compartmentalized cancer drug discovery targeting mitochondrial Hsp90 chaperones. Oncogene *28*, 3681–3688.

Kang, B.H., Plescia, J., Dohi, T., Rosa, J., Doxsey, S.J., and Altieri, D.C. (2007). Regulation of tumor cell mitochondrial homeostasis by an organelle-specific Hsp90 chaperone network. Cell *131*, 257–270.

Keith, B., Johnson, R.S., and Simon, M.C. (2012). HIF1α and HIF2α: sibling rivalry in hypoxic tumour growth and progression. Nat. Rev. Cancer *12*, 9–22.

Lemarie, A., and Grimm, S. (2011). Mitochondrial respiratory chain complexes: apoptosis sensors mutated in cancer? Oncogene *30*, 3985–4003.

Levine, A.J., and Puzio-Kuter, A.M. (2010). The control of the metabolic switch in cancers by oncogenes and tumor suppressor genes. Science *330*, 1340–1344.

MacKenzie, E.D., Selak, M.A., Tennant, D.A., Payne, L.J., Crosby, S., Frederiksen, C.M., Watson, D.G., and Gottlieb, E. (2007). Cell-permeating alpha-ketoglutarate derivatives alleviate pseudohypoxia in succinate dehydrogenase-deficient cells. Mol. Cell. Biol. *27*, 3282–3289.

Petros, J.A., Baumann, A.K., Ruiz-Pesini, E., Amin, M.B., Sun, C.Q., Hall, J., Lim, S., Issa, M.M., Flanders, W.D., Hosseini, S.H., et al. (2005). mtDNA mutations increase tumorigenicity in prostate cancer. Proc. Natl. Acad. Sci. USA *102*, 719–724.

Puisségur, M.P., Mazure, N.M., Bertero, T., Pradelli, L., Grosso, S., Robbe-Sermesant, K., Maurin, T., Lebrigand, K., Cardinaud, B., Hofman, V., et al. (2011). miR-210 is overexpressed in late stages of lung cancer and mediates mitochondrial alterations associated with modulation of HIF-1 activity. Cell Death Differ. *18*, 465–478.

Rasola, A., and Bernardi, P. (2007). The mitochondrial permeability transition pore and its involvement in cell death and in disease pathogenesis. Apoptosis *12*, 815–833.

Rasola, A., Sciacovelli, M., Chiara, F., Pantic, B., Brusilow, W.S., and Bernardi, P. (2010a). Activation of mitochondrial ERK protects cancer cells from death through inhibition of the permeability transition. Proc. Natl. Acad. Sci. USA *107*, 726–731.

Rasola, A., Sciacovelli, M., Pantic, B., and Bernardi, P. (2010b). Signal transduction to the permeability transition pore. FEBS Lett. *584*, 1989–1996.

Selak, M.A., Armour, S.M., MacKenzie, E.D., Boulahbel, H., Watson, D.G., Mansfield, K.D., Pan, Y., Simon, M.C., Thompson, C.B., and Gottlieb, E. (2005). Succinate links TCA cycle dysfunction to oncogenesis by inhibiting HIF-alpha prolyl hydroxylase. Cancer Cell *7*, 77–85.

Semenza, G.L. (2010a). Defining the role of hypoxia-inducible factor 1 in cancer biology and therapeutics. Oncogene *29*, 625–634.

Semenza, G.L. (2010b). HIF-1: upstream and downstream of cancer metabolism. Curr. Opin. Genet. Dev. *20*, 51–56.

Tennant, D.A., Frezza, C., MacKenzie, E.D., Nguyen, Q.D., Zheng, L., Selak, M.A., Roberts, D.L., Dive, C., Watson, D.G., Aboagye, E.O., and Gottlieb, E. (2009). Reactivating HIF prolyl hydroxylases under hypoxia results in metabolic catastrophe and cell death. Oncogene *28*, 4009–4021.

Vander Heiden, M.G., Cantley, L.C., and Thompson, C.B. (2009). Understanding the Warburg effect: the metabolic requirements of cell proliferation. Science *324*, 1029–1033.

Vousden, K.H., and Ryan, K.M. (2009). p53 and metabolism. Nat. Rev. Cancer *9*, 691–700.

Warburg, O. (1956). On the origin of cancer cells. Science *123*, 309–314.

Warburg, O., Wind, F., and Negelein, E. (1927). The Metabolism of Tumors in the Body. J. Gen. Physiol. *8*, 519–530.

Wittig, I., and Schägger, H. (2008). Features and applications of blue-native and clear-native electrophoresis. Proteomics *8*, 3974–3990.

Xie, Q., Wondergem, R., Shen, Y., Cavey, G., Ke, J., Thompson, R., Bradley, R., Daugherty-Holtrop, J., Xu, Y., Chen, E., et al. (2011). Benzoquinone ansamycin 17AAG binds to mitochondrial voltage-dependent anion channel and inhibits cell invasion. Proc. Natl. Acad. Sci. USA *108*, 4105–4110.